

STRAIN ENERGY DENSITY DISTRIBUTION OF VERTEBRAL BODY OF TWO MOTION SEGMENT MODEL UNDER COMBINED COMPRESSION AND SAGITTAL BENDING MOMENT – AN IN VITRO PORCINE SPINE BIOMECHANICAL STUDY

Jaw-Lin Wang*, Yuan-Chuan Tsai, and Been-Der Yang

ABSTRACT

The purpose of the current study is to find the strain energy density (SED) distribution of a vertebral body during different compression loadings, combined with sagittal bending moments. The combined flexion and extension, which are generated by applying an eccentric pointed loading on the motion segment, is to mimic different postures of trunk and loading on the spine. Two strain gage rosettes were applied at an anterior site and a posterior site of a vertebral body. The total SED, deviatoric SED and dilatation SED were obtained from the measurements of the two rosettes. Three major phenomena are observed in the current study; first, the anterior site on the vertebra is at higher risk compared to the posterior site on the vertebra when the motion segment is in compression combined with extreme flexion and extension. Second, the SED is minimal when the loading is applied along the trajectories of the spinal canal and joint facets. Third, the major contribution to SED is from the deviatoric SED. The distribution of SED within the vertebral body during different loading conditions can serve as the baseline for treatment to protect the vertebral body from the risk of compression fracture.

Key Words: strain energy density, vertebral body, spine biomechanics.

I. INTRODUCTION

The principle of traditional spinal fixation instruments is to provide strong fixation and stability of two adjacent moving vertebral bodies. That is to restore the posture and stiffness to the before trauma state. It is hence essential to find the normal posture and stiffness of intact motion segment. The well-recognized method of evaluating the spine function is to apply the pure moment on the motion segment, and then measure the relative rotation of two vertebrae. Larger relative rotation indicates less stability, and vice versa (Abumi *et al.*, 1989; Panjabi, 1988; Panjabi

et al., 1988; Wilke *et al.*, 1998). Although this evaluation method is straightforward, it only provides the global biomechanical behavior of the motion segment. The traditional stability test cannot differentiate as well as newly developed techniques, for instance, the percutaneous vertebroplasty (PV) treatment, which is used to recover the strength of vertebra. The local biomechanical responses, e.g. bone strain, stress and strain energy density (SED), are crucial in differentiating subtle changes with respect to treatment. It is therefore important to find the normal condition of the abovementioned properties of the vertebral body as the baseline for the study of future innovative treatment.

The strain gage implantation on the surface of bone has been widely used for the study of in vivo loading and bone growth and adaptation (Burr *et al.*, 1985; Burr *et al.*, 1989a; Burr *et al.*, 1989b; Lanyon and Rubin, 1984; Rubin and Lanyon, 1984). The strain gage rosettes can also be used to measure the strain

*Corresponding author. (Tel: 886-2-33665269; Fax: 886-2-23687573; Email: jlwang@ntu.edu.tw)

J. L. Wang, Y. C. Tsai, and B. D. Yang are with the Institute of Biomedical Engineering, College of Medicine and College of Engineering, National Taiwan University, Taipei, Taiwan 106, R.O.C.

field and calculate SED. An *in vivo* measurement of a human tibia showed that the SED reached 0.5 kJ/m^3 and 5.5 kJ/m^3 during walking and jogging, respectively (Mikic and Carter, 1995). In addition, they found, during a gait cycle, the majority contribution of SED at heel-off stage came from the shear SED. A maximum of 54 kJ/m^3 SED was found on the equine third metacarpal midshaft throughout the stance and swing phase (Gross *et al.*, 1992). Nevertheless, the application of strain gages to spine biomechanics has before been limited to the measurement of strain on the vertebral body (Frei *et al.*, 2002; Frei *et al.*, 2001; Hongo *et al.*, 1999; Shah *et al.*, 1978) and the contact force on the facet joint (Buttermann *et al.*, 1991; Buttermann *et al.*, 1992) only. The strain measurement on a vertebral body was used to find the stress concentration on vertebral bodies during impact burst fractures (Hongo *et al.*, 1999). Hongo *et al.* attached 11 gages on the cortical bone surface, and applied axial compressive loading on the top of the vertebral body. They found the posterior site of the vertebra was the most critical site for burst fracture injury.

The aim of the current study is to find the distribution of SED on vertebral bodies during different compression loadings combined with sagittal bending moments. The motion segment is point compressive loaded to mimic the motion segment at different postures or rehabilitation strategies. For example, when the point load is applied along the trajectory of the anterior wall of vertebral body, it mimics combined flexion loading together with compressive loading. When the load is applied along the trajectory of the posterior process, it mimics the combined extension together with compressive loading. In this study, we are interested in compression fracture injuries, hence, the total SED, together with the deviatoric and volumetric SED at anterior and posterior sites are measured. It is hoped we can find subtle changes in the vertebral body during different loading conditions. The findings of the current study can serve as the baseline for future studies to find the ultimate treatment for the augmentation of vertebral bodies, such as the PV.

II. METHODS AND MATERIALS

Eight fresh-frozen porcine spinal motion segments (T9-T11, T11-T13) were used in the experiment. The specimens were dissected preserving the osteoligamentous structure. A "drop-tower type" impact testing apparatus was modified for the testing (Fig. 1). The energy, which was generated from the top of the impactor, was transmitted to the specimen through the impounder. The shock absorber was placed on the top of the impounder to control the loading contact period. The stiffness of the shock

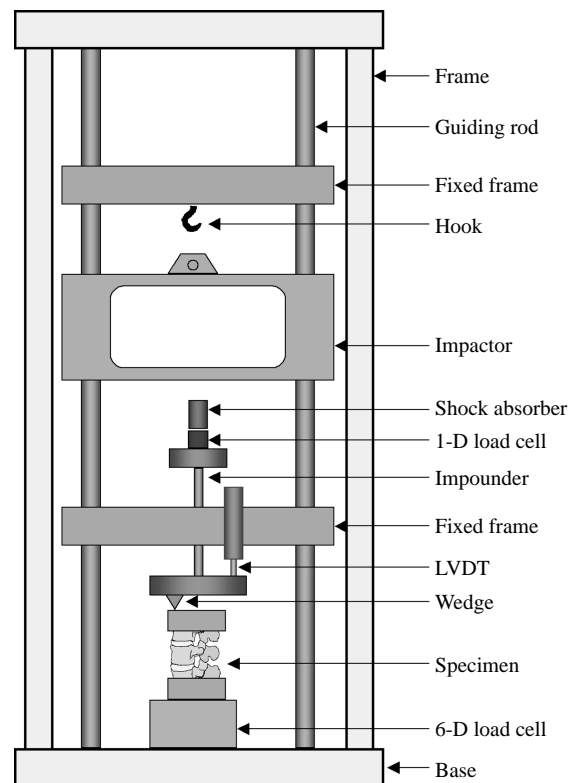


Fig. 1 Continuous Impact Testing Apparatus (CITA). The impactor is guided by two rods to give a vertical motion. The specimen is mounted vertically below the impounder and above the six-axial force load cell.

absorber was 180 kN/m when the loading speed was 1.4 m/sec . The shock absorber was able to give, approximately, contact times of 40 mini-seconds when testing a standard rubber bar specimen (Stiffness = 1000 kN/m , Length = 110 mm) at 12 kg impact mass and 50 mm impact height. The fixed frame, fixed to the guiding rod, was used to align the vertical movement of the impounder. The specimen was mounted vertically below the impounder and above the six-axial force load cell (AMTI MC6-6-4000, Advanced Mechanical Technology, Inc., Watertown, MA, USA).

The specimen was loaded at eight points of location from anterior to posterior. Loading point spacing was 10 mm . The trajectory of the vertical loading of point 1 is along the anterior wall of the vertebral body, while that of point 2 enters the central of the vertebral body. The loading trajectory of point 3 is along the posterior wall, and that of point 4 and 5 go through the spinal canal and the facet joint. The trajectories of points 6, 7 and 8 go through the posterior process (Table 1 and Fig. 2). The loading height is 10 mm , and the weight is 12 kg ; hence the input energy is 1.2 J . Two 3-axial strain gage rosettes (Kyowa KFG-1-120-D17-11N50C2, Kyowa Electronics Instruments

Table 1 Anatomic landmarks of point of loading locations

Point	1	2	3	4	5	6	7	8
Anatomic landmark	Anterior	Center	Posterior	Spinal	Facet		Posterior	
		Vertebral body		cannel	joint		process	

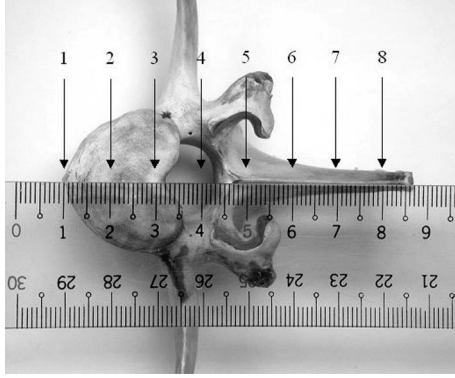


Fig. 2 Locations of loading points on the motion segment

Co., Ltd., Tokyo, Japan) were applied at anterior and posterior sites of the vertebral body (Fig. 3). Signals of two strain gage rosettes, resultant axial forces and flexion moments were recorded at 10 kHz sampling frequency. The signals were then low pass filtered at 500 Hz frequency using Butterworth filtering algorithm.

The two principal strains at anterior and posterior sites of the vertebral body can be calculated from the measurements of the two strain gage rosettes. We assumed the stress-strain field of the vertebral body to be the plain strain, and the stress normal to the surface can also be calculated.

$$\sigma_1 = E \left[\frac{\epsilon_A + \epsilon_C}{2(1-\nu)} + \frac{1}{2(1+\nu)} \sqrt{(\epsilon_A - \epsilon_C)^2 + (2\epsilon_B - \epsilon_A - \epsilon_C)^2} \right]$$

$$\sigma_2 = E \left[\frac{\epsilon_A + \epsilon_C}{2(1-\nu)} - \frac{1}{2(1+\nu)} \sqrt{(\epsilon_A - \epsilon_C)^2 + (2\epsilon_B - \epsilon_A - \epsilon_C)^2} \right]$$

$$\sigma_3 = \nu(\sigma_1 + \sigma_2)$$

The total, dilatation and deviatoric SED hence can be obtained from the principal stresses and stress invariant using the following equations.

$$I_1 = \sigma_1 + \sigma_2 + \sigma_3$$

$$I_2 = \sigma_1\sigma_2 + \sigma_1\sigma_3 + \sigma_2\sigma_3$$

$$I_3 = \sigma_1\sigma_2\sigma_3$$

$$SED_{total} = \frac{1}{2E} [I_1^2 - 2(1+\nu)I_2]$$

$$SED_{dilatation} = \frac{1-2\nu}{6E} (\sigma_1 + \sigma_2 + \sigma_3)^2$$

$$SED_{deviatoric} = SED_{total} - SED_{dilatation}$$

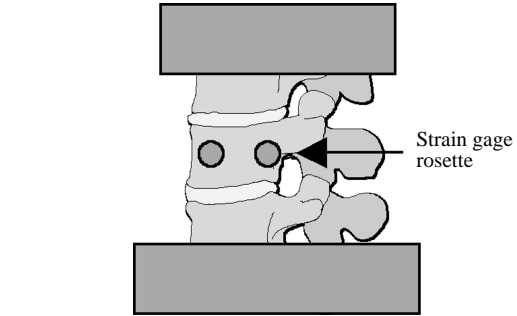


Fig. 3 Locations of strain gage rosettes on the vertebral body

We set the $E=11.032$ GPa, and $\nu=0.3$ for cortical bone (Cao *et al.*, 2001). The stiffness of cortical bone is assumed to be isometric.

III. RESULTS

The typical loading history of axial force and bending moment of point 1 (anterior of vertebral body), point 4 (spinal canal), and point 7 (posterior process) of specimen #11 are plotted in Fig. 4. The contact time of loading is controlled within 50 milliseconds. The peak force reaches around 500 N for this specimen. No significant pattern or magnitude variation of the axial force is found from the changing of loading points (Fig. 4a). The pattern of bending moment, however, changes with the location of loading points. The moment is in flexion when the load is applied at the anterior of the vertebral body, and is in extension when the load is applied at the posterior process of the motion segment (Fig. 4b). The maximum magnitude of axial force and bending moment of each loading with respect to the location of loading points is plotted in Fig. 5. The variation of magnitude of axial force is about constant for all loading location points. The bending moment is in flexion when the load is applied along the trajectory of the anterior and the center of the vertebra. The

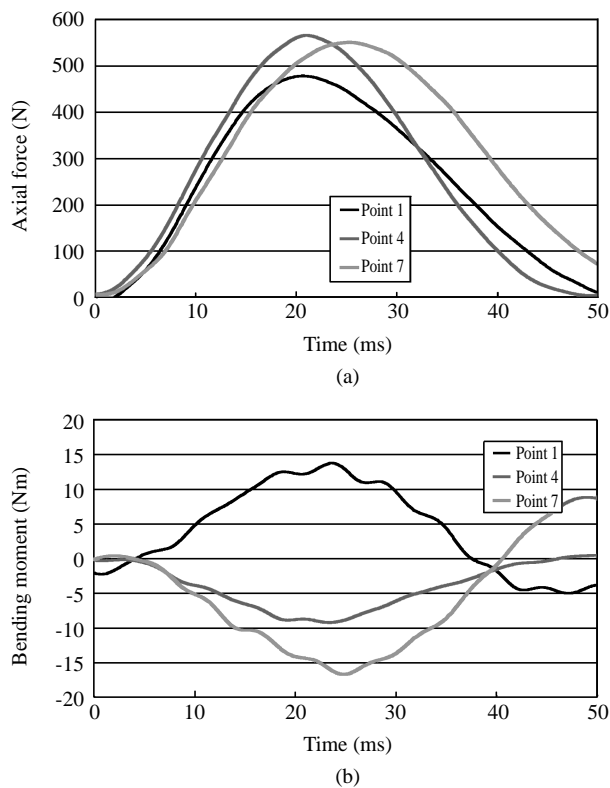


Fig. 4 Typical loading histories of (a) axial force and (b) bending moment of specimen loaded at point 1 (anterior of vertebral body), point 4 (spinal canal), and point 7 (posterior process).

bending moment is about zero when the load is applied along the trajectory of the posterior of the vertebra. The extension moment increases as the loading point moves toward the spinal canal and facet joint. However; the bending moment slightly decreases if the loading moves further to the posterior site of the posterior process.

The total, deviatoric and dilatation SED at both anterior and posterior sites are highest when the load is applied at the anterior wall of the vertebral body (point 1) and the very last location of the posterior process (point 8), that is, the extreme loading condition of axial loading, combined with flexion and extension. The SEDs decrease when the loading point gradually approaches the center of the motion segment. All the SEDs are smallest when the loading is applied along the spinal canal (point 4) and facet joint (point 5). This may indicate that the vertebra is at least risk when the loading is applied at the center of the motion segment, i.e. the trajectory of the spinal canal and facet joint, but not the center of the vertebra. During the extreme loading condition; i.e. the loading points 1, 2, 7, 8; the SEDs at the anterior site of the vertebra are higher than at the posterior site, which may indicate that, the anterior site of the

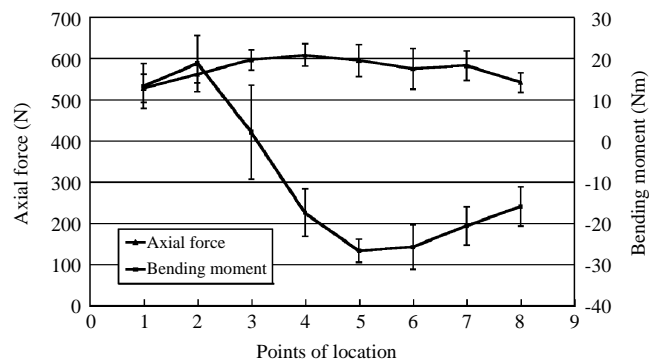


Fig. 5 Peak axial force and the flexion bending moment with respect to the location of loading point

vertebra encounters more risk than the posterior site when the motion segment is at extreme flexion and extension. The highest total SED is at the order of 10 kJ/m^3 , and the lowest total SED is at the order of 1 kJ/m^3 when the input energy of the specimen is 1.2 J (Fig. 6).

More than 50% of the total SED is contributed by the deviatoric SED. At the anterior site of the vertebral body, the contribution of deviatoric SED to the total SED is uniformly and slightly above 70% for all loading location points. At the posterior site of the vertebral body, the contribution of deviatoric SED, nevertheless, is smaller when the load is applied at the anterior wall of the vertebra, i.e. around 50%, but gradually increases when the load is applied at the posterior process, i.e. well above 80% (Fig. 7).

IV. DISCUSSION

To our knowledge, this is the first time that the SED distribution of vertebra with respect to the loading condition has been measured. Our results are in the scale of single digit of kJ/m^3 , which is consistent with *in vivo* SED of human tibia cortex during walking. The input energy of our experiment is only 1.2 J , which is considerably smaller than the *in vivo* condition. However, since the cross section area and height of the specimen are estimated at 2000 mm^2 and 100 mm , and the total volume is in the range of $2 \times 10^{-4} \text{ m}^3$. Assuming the average SED within the vertebra to be 5 kJ/m^3 . This gives the stored energy within the specimen to be 1 J , which is consistent with the scale of input energy. The estimation, therefore, closely matched our data.

Three major phenomena are observed in the current study; first, the anterior site of the vertebra is at higher risk compared to the posterior site of the vertebra when the motion segment is in compression combined with extreme flexion and extension. Second, the SED is minimal when the loading is applied along

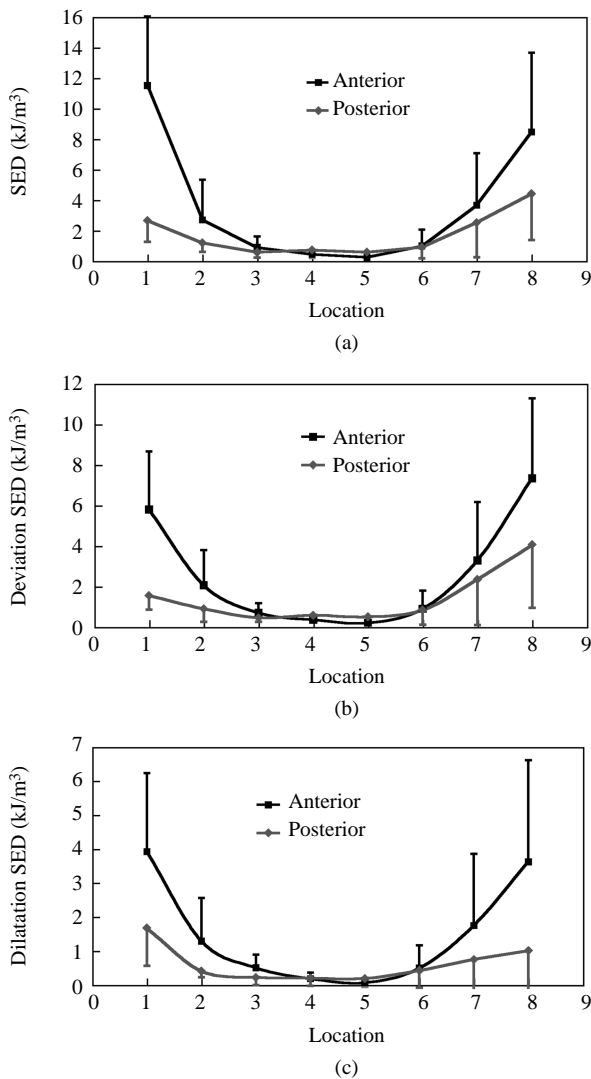


Fig. 6 (a) Total SED; (b) deviatoric SED; (c) dilatation SED of vertebral body at anterior and posterior site with respect to the location of loading points

the trajectories of spinal canal and facet joint. Third, the major contribution of SED is from the deviatoric SED. The first phenomenon is consistent with the pathological observation of vertebra compression fracture, i.e. the collapse of the anterior vertebral body. The second phenomenon may indicate that the straight posture, in which the gravity line of loading trajectory passes through the center of the motion segment, is best at minimizing the risk of compression fracture of the vertebral body. The third phenomenon may imply that the collapse of the anterior wall of the vertebra could be an analogue to the ductile fracture observed in engineering material.

It should be noted that; although we used the impact testing apparatus to conduct the experiment, the current simulation is not for simulation of burst fractures of vertebrae, which is another common

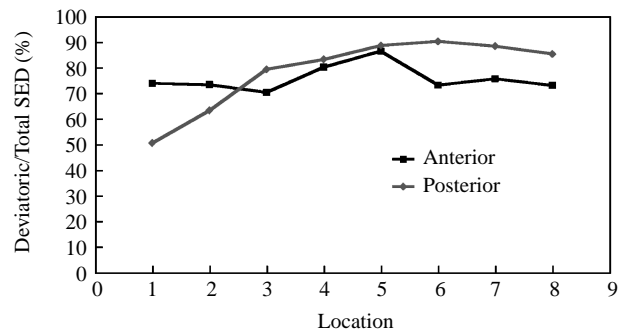


Fig. 7 Ratio of deviatoric SED over total SED of vertebral body at anterior and posterior site with respect to the location of loading point

vertebra deformity observed during accidental injury. The major difference of simulation of the two fractures is the configuration of loading condition. The current loading condition is axial point loading on the top of the vertebra. The motion segment is free to rotate in the sagittal plane. During the burst fracture, the occurrence of the injury is so fast, the rotation of the motion segment in sagittal plane is limited. Hence the simulation of burst fractures is, in general, distributed loaded with constrained rotation in the sagittal plane (Oda and Panjabi, 2001; Oda et al., 2001; Panjabi et al., 2001b; Panjabi et al., 2000). The current protocol is designed to simulate the effect of posture, rehabilitation strategies and daily physiological activities.

In-vitro experiments have used both human and animal materials. The advantage of using the animal model is the consistency of specimen condition that often leads to only small variation of results in experiments. Animal data is widely used for instrumentation calibration (Allan et al., 1990; Nasca et al., 1990; Panjabi 1998; Rikhray et al., 1999). The calf (Allan et al., 1990; Davies et al., 1984; Wilke et al., 1997; Wilke et al., 1996), swine (Allan et al., 1990; Davies et al., 1984) and sheep (Davies et al., 1984; Wilke et al., 1997) are generally used for in-vitro spine biomechanical testing. The advantage of using the human specimen is that the results reflect the human spine behaviors. However, research with human specimens generally uses few specimens, and the condition of the specimens varies a lot due to the lack of control for subject's age, gender ... etc. The large variation in human specimen tests is not good for statistical analysis; however, it is useful to interpret the results, which show the spectrum of mechanical behavior of human specimens (Panjabi, 1998). The biomechanical differences of animals from human specimens include material properties and structural morphology.

In this study, we used porcine spine's. The average bone mineral density (BMD) of tested porcine

vertebral bodies was 1.3 g/cm^2 tested by dual-energy x-ray absorptiometry (Dexa) scanning. In the literature, the BMD of 92 kg and 120 kg porcine spine ranges from 1.107 to 1.165 g/cm^2 (Mitchell *et al.*, 2001). In humans, the average value of Chinese female from 20 to 50 years of age surveyed at National Taiwan University Hospital range from 1.102 to 1.012 g/cm^2 . Our results from porcine vertebra may represent healthy adults before aging.

Compared to other experimental animals such as calves, sheeps, rabbits, rat, ... etc, the morphology of porcine lumbar spine is most analogous to the human spine in terms of morphology (McLain *et al.*, 2002). The most significant morphological difference is the structure of the anterior facet joint (analogous to the superior facet joint in a human spine), which is a "hook" like process (Fig. 8) in comparison to the straight process in a human spine. Although this geometric difference may cause higher facet joint load sharing, especially lateral shear loading, the loading condition of our testing is axial compression only. Hence, we believe that the effect of the morphological difference in such loading is minimal.

We do not consider the effect of muscle recruitment in this study. Some researchers have tried to find spinal physiological loading by putting the load cell into the internal fixation instrumentation (Graichen *et al.*, 1996; Rohlmann *et al.*, 1994; Rohlmann *et al.*, 1998; Rohlmann *et al.*, 2000); however, the data is not conclusive. Recently, follower loads, provided by a tensioned cable along the axis of the spinal column, is designed to mimic the stability effect of the muscle (Cripton *et al.*, 2000; Miura *et al.*, 2002; Panjabi *et al.*, 2001a; Patwardhan *et al.*, 2000; Patwardhan *et al.*, 1999; Patwardhan *et al.*, 2001; Rohlmann *et al.*, 2001). In our current study, we focused on the effect of axial compressive loading and combined flexion and extension. The effects of other directions of forces and moments are minimal.

Spine testing apparatus can be categorized into functional (stability) testing apparatus and the traumatic testing apparatus. The purpose of functional testing apparatus is to mimic the physiological loading condition of the human body. The static loading magnitude of the in-vitro testing of lumbar spine is well recognized, e.g. 7.5 to 10 Nm for flexion moment (Panjabi, 1988; Panjabi, *et al.*, 1988; Wilke, *et al.*, 1998), and 800 N to 2 kN for axial loading (Nachemson, 1981). The purpose of trauma testing apparatus is to mimic various trauma conditions resulting from accidental, occupational or sports injury, e.g. burst fractures of thoracolumbar spines (Oda and Panjabi, 2001; Oda *et al.*, 2001; Panjabi, *et al.*, 2001b), whiplash injuries to cervical spine (Panjabi,

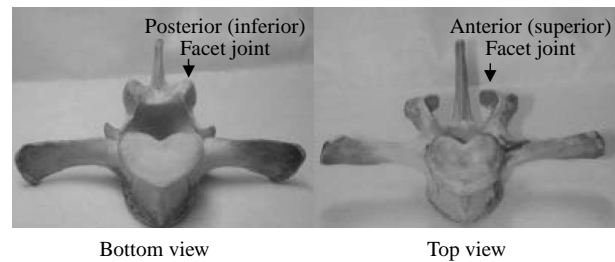


Fig. 8 Bottom view and top view of porcine vertebra

et al., 1998a; Panjabi, *et al.*, 1998b; Panjabi, *et al.*, 2004), and repetitive trauma injury to lumbar spine (Au, *et al.*, 2001; Yoganandan, *et al.*, 1994). Hence the loading magnitude of traumatic testing is of a higher order than functional testing loading. We used vertical point loading to generate complex axial loading combined with sagittal bending moments, using the impact testing apparatus developed at our laboratory. In the current test, the highest magnitude of axial loading is at 600 N , 20 Nm flexion and 25 Nm extension, which are within the range of physiological testing, but not traumatic testing. This magnitude fits the purpose of simulating a motion segment at different postures and rehabilitation strategies.

ACKNOWLEDGMENTS

We appreciate the support from National Science Council of Taiwan, the Republic of China (NSC 92-2320-B-002-103).

REFERENCES

- Abumi, K., Panjabi, M., and Duranceau, J., 1989, "Biomechanical Evaluation of Spinal Fixation Devices. III. Stability Provided by Six Spinal Fixation Devices and Interbody Bone Graft," *Spine*, Vol. 14, pp. 1249-1255.
- Allan, D. G., Russell, G. G., Moreau, M. J., Raso, V. J., and Budney, D., 1990, "Vertebral End-Plate Failure in Porcine and Bovine Models of Spinal Fracture Instrumentation," *Journal of Orthopaedic Research*, Vol. 8, No. 1, pp. 154-156.
- Au, G., Cook, J., and McGill, S. M., 2001, "Spinal Shrinkage during Repetitive Controlled Torsional, Flexion and Lateral Bend Motion Exertions," *Ergonomics*, Vol. 44, No. 4, pp. 373-381.
- Burr, D. B., Martin, R. B., Schaffler, M. B., and Radin, E. L., 1985, "Bone Remodeling in Response to in vivo Fatigue Microdamage," *Journal of Biomechanics*, Vol. 18, No. 3, pp. 189-200.
- Burr, D. B., Schaffler, M. B., Yang, K. H., Lukoschek,

- M., Sivaneri, N., Blaha, J. D., and Radin, E. L., 1989a, "Skeletal Change in Response to Altered Strain Environments: is Woven Bone a Response to Elevated Strain?," *Bone*, Vol. 10, No. 3, pp. 223-233.
- Burr, D. B., Schaffler, M. B., Yang, K. H., Wu, D. D., Lukoschek, M., Kandzari, D., Sivaneri, N., Blaha, J. D., and Radin, E. L., 1989b, "The Effects of Altered Strain Environments on Bone Tissue Kinetics," *Bone*, Vol. 10, No. 3, pp. 215-221.
- Buttermann, G. R., Kahmann, R. D., Lewis, J. L., and Bradford, D. S., 1991, "An Experimental Method for Measuring Force on the Spinal Facet Joint: Description and Application of the Method," *Journal of Biomechanical Engineering*, Vol. 113, No. 4, pp. 375-386.
- Buttermann, G. R., Schendel, M. J., Kahmann, R. D., Lewis, J. L., and Bradford, D. S., 1992, "In vivo Facet Joint Loading of the Canine Lumbar Spine," *Spine*, Vol. 17, No. 1, pp. 81-92.
- Cao, K. D., Grimm, M. J., and Yang, K. H., 2001, "Load Sharing Within a Human Lumbar Vertebral body Using the Finite Element Method," *Spine*, Vol. 26, No. 12, pp. E253-260.
- Cripton, P., Bruehlmann, S., Orr, T., Oxland, T., and Nolte, L., 2000, "In vitro Axial Preload Application during Spine Flexibility Testing: Towards Reduced Apparatus- Related Artefacts.," *Journal of Biomechanics*, Vol. 33, No. 12, pp. 1559-1568.
- Davies, A. S., Tan, G. Y., and Broad, T. E., 1984, "Growth Gradients in the Skeletons of Cattle, Sheep and Pigs," *Anatomia, Histologia, Embryologia: Veterinary Medicine Series C*, Vol. 13, No. 3, pp. 222-230.
- Frei, H., Oxland, T. R., and Nolte, L. P., 2002, "Thoracolumbar Spine Mechanics Contrasted under Compression and Shear Loading," *Journal of Orthopaedic Research*, Vol. 20, No. 6, pp. 1333-1338.
- Frei, H., Oxland, T. R., Rathonyi, G. C., and Nolte, L. P., 2001, "The Effect of Nucleotomy on Lumbar Spine Mechanics in Compression and Shear Loading," *Spine*, Vol. 26, No. 19, pp. 2080-2089.
- Graichen, F., Bergmann, G., and Rohlmann, A., 1996, "Patient Monitoring System for Load Measurement with Spinal Fixation Devices," *Medical Engineering and Physics*, Vol. 18, No. 2, pp. 167-174.
- Gross, T. S., McLeod, K. J., and Rubin, C. T., 1992, "Characterizing Bone Strain Distributions in vivo Using Three Triple Rosette Strain Gages," *Journal of Biomechanics*, Vol. 25, No. 9, pp. 1081-1087.
- Hongo, M., Abe, E., Shimada, Y., Murai, H., Ishikawa, N., and Sato, K., 1999, "Surface Strain Distribution on Thoracic and Lumbar Vertebrae under Axial Compression. The Role in Burst Fractures," *Spine*, Vol. 24, No. 12, pp. 1197-202.
- Lanyon, L. E., and Rubin, C. T., 1984, "Static vs Dynamic Loads as an Influence on Bone Remodelling," *Journal of Biomechanics*, Vol. 17, No. 12, pp. 897-905.
- McLain, R. F., Yerby, S. A., and Moseley, T. A., 2002, "Comparative Morphometry of L4 Vertebrae: Comparison of Large Animal Models for the Human Lumbar Spine," *Spine*, Vol. 27, No. 8, pp. E200-206.
- Mikic, B., and Carter, D. R., 1995, "Bone Strain Gage Data and Theoretical Models of Functional Adaptation," *Journal of Biomechanics*, Vol. 28, No. 4, pp. 465-469.
- Mitchell, A. D., Scholz, A. M., and Pursel, V. G., 2001, "Total Body and Regional Measurements of Bone Mineral Content and Bone Mineral Density in Pigs by Dual Energy X-ray Absorptiometry," *Journal of Animal Science*, Vol. 79, No. 10, pp. 2594-2604.
- Miura, T., Panjabi, M., and Cripton, P., 2002, "A Method to Simulate in vivo Cervical Spine Kinematics Using in vitro Compressive Preload.," *Spine*, Vol. 27, pp. 43-48.
- Nachemson, A., 1981, "Disc Pressure Measurements," *Spine*, Vol. 6, pp. 93-97.
- Nasca, R. J., Lemons, J. E., Walker, J., and Batson, S., 1990, "Multiaxis Cyclic Biomechanical Testing of Harrington, Luque, and Drummond Implants," *Spine*, Vol. 15, No. 1, pp. 15-20.
- Oda, T., and Panjabi, M. M., 2001, "Pedicule Screw Adjustments Affect Stability of Thoracolumbar Burst Fracture," *Spine*, Vol. 26, No. 21, pp. 2328-2333.
- Oda, T., Panjabi, M. M., and Kato, Y., 2001, "The Effects of Pedicle Screw Adjustments on the Anatomical Reduction of Thoracolumbar Burst Fractures," *European Spine Journal*, Vol. 10, No. 6, pp. 505-511.
- Panjabi, M., 1988, "Biomechanical Evaluation of Spinal Fixation Devices. I. A Conceptual Framework," *Spine*, Vol. 13, pp. 1129-1134.
- Panjabi, M., Abumi, K., Duranceau, J., and Crisco, J., 1988, "Biomechanical Evaluation of Spinal Fixation Devices. II. Stability Provided by Eight Internal Fixation Devices," *Spine*, Vol. 13, No., pp. 1135-1140.
- Panjabi, M., Miura, T., Cripton, P., Wang, J., Nain, A., and DuBois, C., 2001a, "Development of a System for in vitro Neck Muscle Force Replication in Whole Cervical Spine Experiments," *Spine*, Vol. 26, No. 20, pp. 2214-2219 S185.
- Panjabi, M. M., 1998, "Cervical Spine Models for Biomechanical Research," *Spine*, Vol. 23, No. 24, pp. 2684-2700.

- Panjabi, M. M., Cholewicki, J., Nibu, K., Grauer, J. N., Babat, L. B., and Dvorak, J., 1998a, "Mechanism of Whiplash Injury," *Clinical Biomechanics*, Vol. 13, No. 4-5, pp. 239-249.
- Panjabi, M. M., Kato, Y., Hoffman, H., and Cholewicki, J., 2001b, "Canal and Intervertebral Foramen Encroachments of a Burst Fracture: Effects from the Center of Rotation," *Spine*, Vol. 26, No. 11, pp. 1231-1237.
- Panjabi, M. M., Kato, Y., Hoffman, H., Cholewicki, J., and Krag, M., 2000, "A Study of Stiffness Protocol as Exemplified by Testing of a Burst Fracture Model in Sagittal Plane," *Spine*, Vol. 25, No. 21, pp. 2748-2754.
- Panjabi, M. M., Nibu, K., and Cholewicki, J., 1998b, "Whiplash Injuries and the Potential for Mechanical Instability," *European Spine Journal*, Vol. 7, No. 6, pp. 484-492.
- Panjabi, M. M., Pearson, A. M., Ito, S., Ivancic, P. C., and Wang, J. L., 2004, "Cervical Spine Curvature during Simulated Whiplash," *Clin Biomech* (Bristol, Avon), Vol. 19, No. 1, pp. 1-9.
- Patwardhan, A., Havey, R., Ghanayem, A., Diener, H., Meade, K., Dunlap, B., and Hodges, S., 2000, "Load Carrying Capacity of the Human Cervical Spine in Compression is Increased under a Follower Load," *Spine*, Vol. 25, No. 12, pp. 1548-1554.
- Patwardhan, A. G., Havey, R. M., Meade, K. P., Lee, B., and Dunlap, B., 1999, "A Follower Load Increases the Load-Carrying Capacity of the Lumbar Spine in Compression," *Spine*, Vol. 24, No. 10, pp. 1003-1009.
- Patwardhan, A. G., Meade, K. P., and Lee, B., 2001, "A Srontal Plane Model of the Lumbar Spine Subjected to a Follower Load: Implications for the Role of Muscles," *Journal of Biomechanical Engineering*, Vol. 123, No. 3, pp. 212-217.
- Rikhranj, I. S., Tan, C. T., Tan, S. K., Teoh, S. H., and Hastings, G. W., 1999, "Use of Titanium Prosthesis to Bridge a Vertebral Gap in the Spine—a Preliminary Experimental Study," *Annals of the Academy of Medicine, Singapore*, Vol. 28, No. 1, pp. 20-24.
- Rohlmann, A., Bergmann, G., and Graichen, F., 1994, "A Spinal Fixation Device for in vivo Load Measurement," *Journal of Biomechanics*, Vol. 27, No. 7, pp. 961-967.
- Rohlmann, A., Bergmann, G., Graichen, F., and Mayer, H. M., 1998, "Placing a Bone Graft More Posteriorly may Reduce the Risk of Pedicle Screw Breakage: Analysis of an Unexpected Case of Pedicle Screw Breakage," *Journal of Biomechanics*, Vol. 31, No. 8, pp. 763-767.
- Rohlmann, A., Bergmann, G., Graichen, F., and Weber, U., 2000, "Changes in the Loads on an Internal Spinal Fixator after Iliac-Crest Autograft," *Journal of Bone and Joint Surgery. British Volume*, Vol. 82, No. 3, pp. 445-449.
- Rohlmann, A., Neller, S., Claes, L., Bergmann, G., and Wilke, H., 2001, "Influence of a Follower Load on Intradiscal Pressure and Intersegmental Rotation of the Lumbar Spine," *Spine*, Vol. 26, No. 24, pp. E557-561.
- Rubin, C. T., and Lanyon, L. E., 1984, "Regulation of Bone Formation by Applied Dynamic Loads," *Journal of Bone and Joint Surgery*, Vol. 66, No. 3, pp. 397-402.
- Shah, J. S., Hampson, W. G., and Jayson, M. I., 1978, "The Distribution of Surface Strain in the Cadaveric Lumbar Spine," *Journal of Bone and Joint Surgery. British Volume*, Vol. 60-B, No. 2, pp. 246-251.
- Wilke, H., Wenger, K., and Claes, L., 1998, "Testing Criteria for Spinal Implants: Recommendations for the Standardization of in Vitro Stability Testing of Spinal Implants," *European Spine Journal*, Vol. 7, pp. 148-154.
- Wilke, H. J., Kettler, A., and Claes, L. E., 1997, "Are Sheep Spines a Valid Biomechanical Model for Human Spines?" *Spine*, Vol. 22, No. 20, pp. 2365-2374.
- Wilke, H. J., Krischak, S., and Claes, L., 1996, "Biomechanical Comparison of Calf and Human Spines," *Journal of Orthopaedic Research*, Vol. 14, No. 3, pp. 500-503.
- Yoganandan, N., Cusick, J. F., Pintar, F. A., Droese, K., and Reinartz, J., 1994, "Cyclic Compression-flexion Loading of the Human Lumbar Spine," *Spine*, Vol. 19, No. 7, pp. 784-790; discussion 791.

**Manuscript Received: May 11, 2004
and Accepted: Aug. 04, 2004**